Architectural *terracruda* sculptures of the Silk Roads: new conservative insights through a diagnostic approach based on non-destructive X-ray micro-tomography

Mònica López-Prat[1], Raffaele Giuseppe Agostino[2], Sudipa Ray Bandyopadhyay[3], Begoña Carrascosa[1], Maria Caterina Crocco[2], Raffaella De Luca[4], Raffaele Filosa[2], Vincenzo Formoso[2], Carla Lancelotti[5, 6], Noor Agha Noori[7], Alessandra Pecci[8], José Simón-Cortés[1], Domenico Miriello[4]

[1]Universitat Politècnica de València, Departament de Conservació i Restauració de Béns Culturals, Valencia, Spain

[2]Università della Calabria, Dipartimento di Fisica and STAR-Lab, Arcavacata di Rende, Italy

[3]University of Calcutta, Department of Ancient Indian History and Culture West Bengal, India

[4]Università della Calabria, Dipartimento di Biologia, Ecologia e Scienze della Terra, Arcavacata di Rende, Italy

[5]Universitat Pompeu Fabra, CaSEs Research Group, Barcelona, Spain

[6]ICREA, passeig Lluís Companys, Barcelona, Spain

[7]Archaeology Institute of Afghanistan, Kabul, Afghanistan

[8]Universitat de Barcelona, ERAAUB Research Group, Barcelona, Spain

Keywords: conservation, *terracruda* sculptures, X-ray microtomography, sculpting technique, ethnographic data

ABSTRACT*:* This work presents the results of the study of a fragment of architectural *terracruda* sculpture from the Buddhist archaeological site of Tepe Narenj (Kabul, Afghanistan, 5th-9th centuries) through X-ray micro-tomographic analysis. This technique offers great potential for the study of artworks that, due

to their nature, state of conservation or relevance, do not allow for destructive analysis. The results have provided useful data for the understanding of the sculpturing methodology, showing for the first time the relevance of materials of plant origin used in the composition of the clay-based modelling pastes, a feature that has not been previously highlighted, and which appears to be crucial for proposing suitable conservation intervention.

1. INTRODUCTION

The practice of modelling architectural *terracruda* sculptures is a very specific artistic technique that presents no known examples outside of South, Central and Eastern Asia. These sculptures, which can be smaller than human size or reach several meters in height, are skilfully modelled in-situ: starting from a core-skeleton of wood, brick or stone joint to the architecture, modelled with different clay-based layers frequently covered with stucco and, finally, gilded and/or polychrome (Varma 1970, Tarzi 1986, Luczanits 2004). Historic examples of this artistic expression are mainly linked to the spread of Buddhist Art from the North-west Indian subcontinent through what is known today as the "Silk Roads". The first Buddhist instances are found, at the beginning of the common era, in the area of present-day Pakistan, Afghanistan, south of Uzbekistan and Tajikistan. Later, they spread to the Himalayas and Eastern Asia, where examples can be identified up to modern times.

Despite their extraordinary interest, this type of sculptures has received little attention from the scientific community dedicated to heritage conservation. The conservation studies carried out so far have usually focused on investigating the mineral and chemical composition of the pastes and polychromies (Bayerová et al. 2010; Blaensdorf and Tao 2010; Lluveras et al. 2011; Singh et al. 2014; Wang et al. 2014; Wang et al. 2020). Conversely, the precise methodology employed to

model sculptures that usually exceed human size and where the use of organic material of plant origin mixed with the clay plays an extremely important role, has been understudied. Two main issues can be identified among the causes of the limited research on these sculptures: either they are still in situ, usually in regions of complex access, or they have already been extensively treated through various recovery measures that have largely changed their morphology. Additional motives may be related to the fact that these sculptures are produced with a modelling technique unknown outside Asia and made of raw or unfired clay, a material that has traditionally been little used in the West for the production of artworks intended to "remain".

In this context, an interdisciplinary collaborative research work is being carried out between the Polytechnic University of Valencia (Spain), the University of Calabria (Italy) and the Archaeological Institute of Afghanistan, with the contribution of the National Geographic Society. The aim is to fully understand the artistic technique used to make architectural *terracruda* sculptures and then explore new conservative treatments more in line with the current premises using ecological and sustainable materials. For this research, we hypothesize that this ancient technique is still used in some areas of India, such as West Bengal, where an ancient caste of artists continues to produce large clay-based sculptures following a century-old tradition described in Sanskrit ritual texts, the oldest dating back to the 8th century CE (López-Prat et al. 2021, in press).

The broader project combines the characterization of the raw materials used in the manufacture of the ancient sculptures with the data obtained during the ethnographic field work. The aim is to compare the elaboration methodology by means of qualitative analysis of archaeological and ethnographic data, as well as geochemical, mineralogical and botanical analysis of samples of clay-based sculptures, both from modern Hindu examples and from fragments collected from a selection of different archaeological sites in Afghanistan preserving in-situ

architectural *terracruda* sculptures. In this regard, although the research is based on the comparison of two extremes of the same technology and there will undoubtedly be variations caused by the time lag and geographic difference, there are clear parallels that point to similar patterns, based on the use of a core of materials with specific properties and applied in predetermined steps, which finally allow the creation of large sculptures of unfired polychrome clay.

In this paper we present the first results of the non-destructive analysis of a sculpture fragment (part of a finger), sample named TN7 (Fig. 1), from the archaeological site of Tepe Narenj (Kabul, Afghanistan). The site, whose current name literally means "Hill of orange trees", is located on the route that connected the historical regions of Gandhara and Bactria or, in other words, India with Central Asia. It lies on the eastern slopes of the Hindukush mountain chain, only a few kilometres south of the current city of Kabul (Fig. 2). According to archaeological research, Tepe Narenj was the location of a Buddhist monastery that was active between the 5th and 9th centuries CE. The field works uncovered an architectural complex system with three levels (lower, middle and upper) interconnected by a system of steps and platforms (Paiman 2017). On the terraces in the middle portion of the site stood a series of cult chapels where the remains of multiple examples of architectural *terracruda* sculptures are preserved (Fig. 3). Tepe-Narenj is today one of the best surviving examples of Afghan Buddhist archaeological complexes, especially because of the importance of the architectural *terracruda* sculptural decoration preserved in-situ.

These sculptures were modelled following the aforementioned technique, which in this case involved the use of a core skeleton of wood, followed by layers of different clay-based plasters and finally covered with a thin layer of white stucco that in some cases retains traces of colour. Even though the sample studied in this work represents only a small part of a whole figure, its analysis is

representative of the technique and the main materials used for the rest of the sculpture that, according to what we know so far, only vary in the proportion between the inert, organic and clay fractions depending on the part of the body being processed. In addition, we hope to be able to reintegrate it to the statue of origin; this implies that during the analytical phase the sample must be preserved without performing destructive operations. However, terracruda materials are very brittle and difficult to treat, even during the phase aimed to investigate the chemical, mineralogical, petrographic and textural composition. Unfortunately, the analytical procedures that allow to obtain detailed compositional information are predominantly destructive, as they require cutting and pulverizing the sample. Thus, X-ray microtomography was outlined as a very suitable technique, although it does not provide chemical or mineralogical information, it is extremely valuable to discover important information on the internal structure of the sample. In addition, it could provide data on the number of layers that conformed the finger, on the distribution and dimensions of the different materials in the different layers, on the possible presence of completely degraded organic materials used in the mixture and on the volumetric distribution of the voids, clayey and inert material in the different layers.

2. Methodology

2.1. Object of the study

Sample TN7 (Fig. 1) is, as mentioned, a fragment of a finger, with maximum length of 21 mm and a diameter of 36 mm. It was recovered from a wicker basket located inside Chapel 5 - Zone III. According to the archaeological interventions, this area belongs to the second period of occupation of the monastery, dated mid-6th century.

2.2. Analytical techniques

Preliminary macro- and microscopic observations with a LEICA-EZ4W microscope was followed by X-ray micro-tomographic analysis (micro-CT). The micro-CT is a non-destructive technique of radiographic imaging, able to produce 3D images of the inner structure of a solid material with a spatial resolution in the order of the micrometers, based on a set of bi-dimensional radiographic images from a sample (Wildenschild 2013; Boerckel 2014). This technique is applied in a vast diversity of fields: medicine, biology, engineering, palaeontology and earth sciences are just few examples. Applied to cultural heritage, the technique has been mainly used for the study of stone and metal artefacts, but also in an exploratory fashion in the technological study of ceramics and bricks (Kahl and Ramminger 2012; Kulkova and Kulkov 2014; Kozatsas et al. 2018; Park et al. 2019; Coletti et al. 2016; Agostino et al 2016; and Reedy 2020). To the best of our knowledge, X-ray microtomography has been only applied unfired clay objects to read the inscriptions on ancient clay tablets that had been sealed in clay envelopes and in the technological study of unfired Neolithic clay figurines from Ancient Near East (Applbaum and Applbaum 2005). However, the use of non-destructive techniques becomes crucial in case of very friable artefacts, like clay-based artefacts, because destructive analyses that break or cut the clay sample to study its various components, contributes to the loss of textural and spatial information (Bukreeva 2016).

The principle of micro-CT is based on the attenuation of X-rays passing through the sample being imaged: as the X-ray passes through a homogeneous object the intensity of the incident X-ray beam is reduced according to the Lambert-Beer equation (Fig. 4):

$$\boldsymbol{I = I_0 e^{-\mu x}}$$

Where $\boldsymbol{I_0}$ is the intensity of the incident beam, $\mathbf{x}$ is the distance covered by the X-ray in the absorbing object and μ is the linear attenuation coefficient (Landis and Keane 2010).

The cone beam microtomography has the advantage to use a simple and versatile apparatus.

In general, a micro-CT system is composed of an X-ray source, a detector, a sample holder, and a process control system by computer for moving the sample, or detector, or X-ray source (Lee et al. 2003). There are also computational systems for the acquisition, processing and reconstruction of tomographic images, to carry out qualitative and quantitative analyzes.

Figure 5 shows a schematic diagram of the operational sequence used to perform an X-ray microtomography measurements. A microtomography apparatus performs an initial measurement rotating the sample on its own axis while the X-ray source and detector remain fixed, or *viceversa*. The microfocus X-ray source continuously irradiates the object (or the sample), while the flat-panel detector acquires a series of 2D projections of the object at different angles with a constant angular step until completing 360 degrees and at a fixed integration time. The angular step (typically a fraction of degree) and integration time are computer-controlled.

Lastly, the 3D digital reconstruction is based on a Filtered Back-Projection algorithm (FBP) (Kak and Slaney 1988). In our case, since the micro-CT apparatus uses an X-ray cone beam source, the 3D digital reconstruction is performed using the algorithm by Feldkamp, Davis, and Kress (FDK) (Feldkamp et al.1984). The 3D digital reconstruction produces a 2D dataset of cross sections perpendicular to the rotation axis, called slices. The stack of slices provides three-dimensional volumetric data. The sample can be then viewed and analysed in a virtual environment in various ways, either by viewing a single slice of the sample or the 3D virtual volume where each volume unit, called voxel, contain information on the X-ray absorption coefficient.

2.3. Experimental setup

The micro-tomographic experimental station used in this work (μTomo- supplied by Sincrotrone Trieste SCPA) is part of the STAR-Lab facility realized under the PON MaTeRiA project. It is located at the University of Calabria in Italy.

The μTomo experimental station, based on a cone beam geometry, used in this analysis, and shown schematically in Figure 6, is composed of:

- a microfocus X-ray source Hamamatsu L12161-07;
- a flat panel detector Hamamatsu C7942SK-05;
- a six degree of freedom sample positioning system (linear movement and rotation stage);
- hardware and software system for control and data acquisition.

All the components except the process control system are mounted on an optical bench. The microfocus X-ray source continuously irradiates the object (or the sample), which is rotated with a constant angular step until completing 360 degrees and the flat-panel detector acquires a series of 2D projections of the object at different angles and at a fixed integration time.

The X-ray source is a polychromatic microfocus X-ray generator (Hamamatsu L12161-07) with a tungsten target. The microfocus source can be operated with a voltage range from 40kV to 150kV and allows three power modes that determine the source size. The minimum source size (5 μm) is obtained at power below 4W. The X-ray cone beam aperture is about 43 degrees.

The detector is a Flat panel sensor C7942SK-05 from Hamamatsu. These detectors are based on two-dimensional arrays of photodiodes CMOS (CCD) directly coupled to a scintillator for X-ray to light conversion. Its main features are shown in the Table 1.

The sample positioning system (by PI miCos Industry) provides six degrees of freedom: three linear motor for x, y, z movement, one for the rotation stage theta (θ) and two stages for tilt angles. This system allows to position the sample with

the required precision. In particular, the Source-to-Object Distance (SOD) and Source-to Detector Distance (SDD) determine the system geometric parameters such as magnification ratio (M=SOD/SDD).

The μTomo station is provided with a user interface that allows its control through a computer. All the electronic hardware components are commercially available and are, in general, provided with software drivers which are LabVIEW compatible (Ionita et al. 2008; Conte et al. 2019).

The sample object of this study was investigated at the μTomo experimental station with the following experiment setup: the X-ray source operated at a voltage of 130kV, a current of 76μA (source power 10 W) and a focal spot size of 7 μm; the low energy components with of the X-ray beam were filtered by 100 μm-thick Copper foil. In this study, the SOD was set to 200mm and the SDD to 500 mm, then the magnification equal to M=2.5. Considering the employed beam magnification, the equivalent voxel side was 20μm. A set of 1800 projections were acquired over an angular range of 360° using a 0.2-degree angular step and an exposure time of 2 s/projection. Axial slices were reconstructed with an isotropic voxel size of 20μm using the FDK algorithm for cone-beam geometry. The measurement parameters are shown in the Table 2.

2.4. 3D image analysis

Image analysis was performed with Fiji (Schindelin et al. 2012) an open source image processing package based on ImageJ. ImageJ is an open source software developed by the National Institutes of Health of the United States, which allows digital image processing operations. ImageJ is designed with an “open architecture” that provides the possibility to install extensions via small subprograms "Java plugin" and the possibility to develop many macros for ad-hoc processing, working on 2D and 3D space.

The aim of the analysis is to retrieve the morphology and topology of the constituents of the sample. The first step consisted in extracting a volume of interest (VOI) from the stack of reconstructed slices. The selected VOI enclosed a representative amount of the sample heterogeneity and can be defined as Representative Elementary Volumes (REVs) (Costanza-Robinson et al 2011). The VOI was filtered with a '3D Gaussian-Blur filter' (Ollion et al. 2013) to reduce the image noise and segmented by an automatic thresholding algorithm (Otsu 1979) to separate the different materials in the sample (clay, sand and voids).

Following the study of the macro structure of the sample, the various components were isolated and analysed separately. The '3D ImageJ Suite' (Ollion et al. 2013) of the Fiji software library was applied to evaluate the density of the different components, which provides their volumetric fraction within the sample. A morphological and topological analysis of clay, sand and voids was performed by excluding those touching the VOI borders, since they can be truncated, and their volume and morphology may not be representative of the real shape. For volumetric analysis, the sample was divided into three parts identified as internal layer, intermediate layer and external layer.

The volume of different components was obtained via the '3D Geometrical measurements' and '3D Object Counter' (Bolte and Cordelières 2007, plugins of Fiji. The 3D visualization was performed by volume rendering procedures using the plugins 'Volume Viewer' (Barthel 2006) and '3D Viewer' (Schmid et al. 2010). This analysis allowed to determine the three-dimensional shape of the clay, sand and voids and their distribution and orientation inside the sample.

3. Results and discussion

The preliminary visual observation allowed to detect that the elaboration of the fragment studied follows the practice documented in technical studies of this type of sculptures (Varma 1970, Tarzi 1986, Luczanits 2004). In fact, it was

observed that the finger was made of superimposed layers of greyish brown (Munsell 10YR 6/3) clayey material, layered around a rigid element (today decomposed) and finished with a thin layer of white stucco only partially preserved. Macropores and impressions left by organic material, most probably of plant origin, mixed with the clayey paste are visible in the section to the naked eye. The identification of the various layers also highlights the different phases of the modelling process and the preparation of layers with different compositions. The first result of the X-ray micro-tomography is shown in Figure 7, where it is possible to observe the 3D rendering of a cylindrical section of the bulk sample (Fig. 7a) and a cut through an oblique plane (Fig. 7b). The three-dimensional reconstruction of the bulk sample from different points of view can be found in the video available in the supplementary material (video 1). The bulk image shows that there are three main layers superimposed around the central cavity. The equatorial section of the sample shows the precise details of the three principal layers (Fig. 8). The inner layer (layer 1), the one closest to the cavity, and the intermediate layer (layer2) have a thickness of c. 5 mm. The outer layer (layer 3) is the thinnest (c. 2 mm). Some fragments of white stucco on the surface are visible on the most external layer, whose thickness is approximately 1.8 mm (Fig. 8).

From the 3D reconstruction of sample TN7 it was possible to segment and perform the thresholding of the three main components of the sample: the clay fraction, the inert material and the voids. The morphology of the voids is very particular; it does not correspond to that usually observed in clayey mixtures. They are not spherical or elliptical but have shapes that fit with traces of decomposed organic material, which is most likely of plant origin. The idea was to perform the thresholding of the voids to reconstruct the morphology of the organic material in three dimensions and verify this hypothesis. Table 3 shows the estimation of the percentage of the clayey material, inert material and voids

in the layers 1, 2 and 3. All three layers are mainly made of clayey material, which it is 92.71% in the layer 1, 87.29% in the layer 2 and 90.38% in the later 3. The 3D reconstruction of the clay fraction is shown in Figure 9. A video with the full three-dimensional reconstruction of the clayey fraction can be found in the supplementary material (video 2). The inert fraction is the least abundant compared to the voids and the clayey fraction; it represents 1.81% of layer 1, 1.64% of layer 2 and 4.53% in layer 3 (Table 3). The mean size of the inert fraction in the three layers is very similar: c. 264 µm in layer 1, 166 µm in layer 2 and 202 µm in layer 3 (Table 3). However, in all three layers it is possible to find rare larger fragments of inert material varying between 1280 and 1660 µm. Figure 10 shows the 3D rendering of the inert material of the sample TN7 from different points of view and a video of the full three-dimensional reconstruction of the inert fraction can be found in the supplementary material (video 3). The cumulative frequency curves of the particle size distribution for the inert material inside layers 1, 2 and 3 are very similar; this suggests that the same inert material have been used for the three layers (Fig. 11). However, it is difficult to establish at this stage if the inert material is naturally present in the clay or if it was added later to reduce the plasticity of the clays. The distinct volumetric content of inert material in the various layers could support the second hypothesis or point to a separate origin for the clay materials in order to obtain different properties related to the plasticity and stickiness of the clay, as shown by some technical studies done on *terracruda* sculptures from the Buddhist temple complex at Nako (Bayerová et al. 2010) and in the ethnographic research done in 2019 in West Bengal (López-Prat et al. 2021, in press). This showed the same principle and noted the employment of two different clays extracted from different places and used mixed or separately depending on the layers or parts to be modelled in the general step-by-step process necessary for the entire creation of a sculpture. These clays are used as needed: one, stickier and harder, the other, sandier and more malleable.

In this sense, the results of the microtomography showing the presence of different amounts of inert materials could indicate similar purposes.

Among all the data obtained from the X-ray micro-tomography, the one relating to voids is perhaps the most interesting and surprising. The three-dimensional segmentation of the voids shows a perfect cast of vegetal material, which is present only in the first two inner layers, while it is completely absent in the third layer (Fig. 12 and 13). In the first layer the voids created by plant material represent about 5.48 % while in the second layer about 11.07% of the layer (Table 3). In the third layer, 5.09% of voids are due to small shrinkage cracks and not to the presence of vegetal material. The voids left by decomposed material can reach a length of 1.5 cm (Fig. 13b) and present diameters ranging from 200 µm to 1.7 mm. (Fig. 13b). In Figures 12 and 13 it is also possible to observe how the voids wind around the central cavity and are oriented in the same direction, which in all probability indicates a modelling process around a central rigid and perishable structure. A video with the full three-dimensional reconstruction of the voids can be found in the supplementary material (video 4). The use of plant-based materials in the inner layers of TN7 shows a clear parallel with the process of modelling fingers in the Bengali sculptures observed during the ethnographic work, which are performed in series separately by adding a large amount of jute fibres to the clay mass (product of the mixture of the two aforementioned clays), to increase its rigidity without adding any internal structure in this case (Fig. 14). Moreover, the absence of voids detected in the outermost layer of TN7, together with the greater presence of inert material, also presents an analogy with current Bengali sculptors, who, in order to finish the modelling process of the different layers of clay, apply a denser and more liquid paste, prepared exclusively with the most sticky clay, to which cotton textiles are adhered. This last layer of clay prepares the sculpture to receive the white stucco coating, necessary to polychrome the sculpture. In the microtomography, the micrometric space left

between layer 3 and the areas where the stucco layer has been preserved (see Fig. 8) might indicate the presence of a similar fabric, now missing but documented in other sculptures on the site (Paiman 2005, 2012).

4. Conclusions

The elaboration of architectural *terracruda* sculptures through the superimposition of various layers of clay mixed with plant-material starting from a rigid skeleton, mirrors a technique documented in multiple Buddhist archaeological sites and historical temples along the Silk Roads, from the north-western part of the Indian subcontinent to Eastern Asia crossing the Himalayas. In this perspective, X-ray microtomography has proved to be of great value in understanding this artistic technique, especially by unravelling in a non-destructive manner the stratigraphy and the proportions between the mineral components and the organic material present in the modelling pastes, mainly decomposed and often disregarded during destructive analyses. As far as we know, this is the first time that an analysis allows to see the high proportion of organic material that was originally added to the clay and that technically made possible to produce large *terracruda* sculptures. Knowing the proportion of organic material is crucial from a conservation point of view, especially for developing compatible treatments in the consolidation and reintegration phases aimed at reproducing grouts to fill gaps and cracks that are light enough, so their weight and the shrinkage caused by drying do not lead to the appearance of new breaks and detachments in the originals.

After this research, the question that arises is what type of plant material was used in ancient times and whether their use was random or whether specific properties were sought, as is the case today in West Bengal, where rice husk and

chopped straw as well as jute fibres are added with particular purposes in almost every stage of the manufacture of a clay-idol. These include stickiness, lightening the weight, facilitate drying avoiding cracks and increasing the rigidity of the clay layers. Finding the right material to reproduce the essential role of the fibres in the modelling process will be an important step towards the complex final objective of preserving architectural *terracruda* sculptures found in archaeological context.

In this sense, within the framework of this research project, phytolith and DNA analyses are being carried out on different samples from various Afghan sites with examples of architectural *terracruda* sculpture. The results are being compared with current Bengali methodology, which has inspired the exploration of the possibilities of adding to clay micronized rice husk as a possible component in the manufacture of compatible and light enough filling mortars in the restoration process.

Acknowledgements

This research is part of Mònica López Prat's ongoing doctoral research conducted in the Polytechnique University of Valencia in collaboration with the University of Calabria and has been supported by a National Geographic Society Early Career Grant (EC-59568C-19). The activity of Carla Lancelotti has been supported by the Generalitat de Catalunya with grant SGD2017-212. The μTomo experimental station was acquired by the PON MaTeRiA project - PONa3_00370 – funds. We gratefully acknowledge Zafar Paiman, who explained the details of his studies in Tepe-Narenj, Susan S. Bean, for always being available to share their knowledge about the tradition of modelling *terracruda* sculpture in southern Asia, and all the Bengali artists (specially the *kumors* of Kumortuli) who, in keeping with their ancient tradition, have collaborated to understand the process of modelling *terracruda* sculptures. Many thanks to all the people and

institutions involved in this transboundary east-west research and specially to an explorer met in Samarkand.

REFERENCES

R.G. Agostino, S. Donato, T. Caruso, E. Colavita, F. Zanini, A. D'Alessio, D. Pisarra, A. Taliano Grasso, Microtomographic studies as a tool in the identification of a new ceramic class: The metal-imitating pottery as grave goods among Brettians and Lucanians, Microchemical Journal, Vol. 126, pg. 138-148, 2016.

N. Applbaum and Y. H. Applbaum "The use of medical computed tomography (CT) imaging in the study of ceramic and clay archaeological artifacts from the Ancient Near East" in M. Uda, G. Demortier, and I. Nakai, eds. X-Rays for Archaeology, p. 231-245. Dordrecht: Springer, 2005.

K. U. Barthel, "3D-data representation with ImageJ," in ImageJ Conference, 2006.

T. Bayerová, M. Gruber and, G. Krist "Technical study of polychrome clay sculptures from the Buddhist temple complex at Nako", in Proceedings of the Sculpture, Polychromy, and Architectural Decoration Working Groups ICOM-CC Interim Meeting: Multidisciplinary Conservation: A Holistic View for Historic Interiors, Rome 2010.

C. Blaensdorf and M. Tao, "A Chinese-German Cooperative Project for the Preservation of the Cultural Heritage of Shaanxi Province: Conservation of the Polychrome Clay Sculpture and Investigation of Painting Materials in the Great Hall of the Shuilu'an Buddhist Temple", in Conservation of Ancient Sites on the Silk Road, The Getty Conservation Institute, p. 203–211, 2010.

J. D. Boerckel, D. E. Mason, A. M. McDermott, and E. Alsberg,"Microcomputed tomography: approaches and applications in bioengineering," Stem Cell Res. Ther., vol. 5, no. 6, p. 144, 2014.

I. Bukreeva, A. Mittone, A. Bravin, G. Festa, M. Alessandrelli, P. Coan, V. Formoso, R. G. Agostino, M. Giocondo, F. Ciuchi, et al. "Virtual unrolling and deciphering of Herculaneum papyri by X-ray phase-contrast tomography," Sci Rep 6, 27227 (2016). https://doi.org/10.1038/srep27227

Bolte and F. P. Cordelières, "A guided tour into subcellular colocalization analysis in light microscopy," J. Microsc., vol. 224, no. 3, p. 213–232, 2006.

C. Coletti, G. Cultrone, L. Maritan and C. Mazzoli, "Combined multi-analytical approach for study of pore system in brick," Materials Characterization, no. 121, p. 82-92, 2016.

T. J. Collins, "ImageJ for microscopy," Biotechniques, vol. 43, no. S1, p. S25-S30, 2007. https://doi.org/10.1111/j.1365-2818.2006.01706.x

R. Conte, R. Filosa, V. Formoso, F. Gagliardi, R. G. Agostino, and G. Ambrogio "Analysis of extruded pins manufactured by friction stir forming for multi-material joining purposes", in AIP Conference Proceedings 2113, 050026, 2019. https://doi.org/10.1063/1.5112590

M. S. Costanza-Robinson, B. D. Estabrook, and D. F. Fouhey, "Representative elementary volume estimation for porosity, moisture saturation, and air-water interfacial areas in unsaturated porous media: Data quality implications" Water Resour. Res., vol. 47, no. 7, 2011. https://doi.org/10.1029/2010WR009655

L. A. Feldkamp, L. C. Davis, and J. W. Kress, "Practical cone-beam algorithm" Josa a, vol. 1, no. 6, p. 612–619, 1984. https://doi.org/10.1364/JOSAA.1.000612

C. N. Ionita, K. R. Hoffmann, D. R. Bednarek, R. Chityala, and S. Rudin, "Cone-beam micro-CT system based on LabVIEW software" J. Digit. Imaging, vol. 21, no. 3, p. 296–305, 2008. https://doi: 10.1007/s10278-007-9024-9

W. A. Kahl and B. Ramminger, "Non-destructive fabric analysis of prehistoric pottery using high-resolution X-ray microtomography," Journal of Archaeological Science, no. 39, p. 2206-2219, 2012.

A. C. Kak and M. Slaney, "Principles of computerized tomographic imaging IEEE Press," New York, 1988.

J. Kozatsas, K. Kotsakis, D. Sagris, and K. David. Inside out: assessing pottery forming techniques with micro-CT scanning. Journal of Archaeological Science, no. 100, p. 102-119. 2018.

M. Kulkova and A. Kulkov, "Investigations of Early Neolithic ceramics from Eastern Europe by X-ray microtomography and petrography," Microscopy and Analysis, no. 136, p. 7-10, 2014.

E. N. Landis and D. T. Keane, "X-ray microtomography," Mater. Charact., vol. 61, no. 12, p. 1305–1316, 2010.

S. C. Lee, H. K. Kim, I. K. Chun, M. H. Cho, S. Y. Lee, and M. H. Cho, "A flat-panel detector based micro-CT system: Performance evaluation for small-animal imaging," Phys. Med. Biol., 2003.

A. Lluveras, I. Bonaduce, M. P. Colombini, C. Blaensdorf, and M. Tao, "A first insight into the Asian clay sculptures painting technique and materials: western and eastern buddha of the Bamiyan valley (Afghanistan) and sculptures from Shuilu'an (Shaanxi province, China)", in Art'11 - 10th International Conference on Non-Destructive Investigations and Microanalysis for the Diagnostics and Conservation of Cultural and Environmental Heritage. Florence, Italy, 2011.

M. López-Prat, "Buddhist Clay Sculptures in Central Asia: Conservation and Restoration Problems", in *Proceedings of the First International Conference on Rammed Earth Conservation (Restapia 21-23 June 2012*, Valencia, Spain), p. 669-673.

M. López-Prat, B. Carrascosa, D. Miriello, J. Simón-Cortés, and S.R. Bandyopadhyay, An ethnographic approach to developing new conservation strategies for the archaeological clay-based sculpture of the Silk Road. In Transcending Boundaries: Integrated Approaches to Conservation. ICOM-CC 19th Triennial Conference Preprints, Beijing, 17–21 May 2021, ed. J. Bridgland. Paris: International Council of Museums (In press).

C. Luczanits, Buddhist Sculpture in Clay. Early Western Himalayan Art, Late 10th to Early 13th Centuries. Serinda Publications, 2004.

Munsell Soil Color Book, 2009 Revised, 2018 Production by Munsell Color X-rite.

J. Ollion, J. Cochennec, F. Loll, C. Escudé, and T. Boudier, "TANGO: a generic tool for high-throughput 3D image analysis for studying nuclear organization," Bioinformatics, vol. 29, no. 14, p. 1840–1841, 2013. https://doi.org/10.1093/bioinformatics/btt276

N. Otsu, "A threshold selection method from gray-level histograms," IEEE Trans. Syst. Man. Cybern., vol. 9, no. 1, p. 62–66, 1979.

Z. Paiman, "La renaissance de l'archéologie afghane. Découvertes à Kaboul" Archeologia, no. 419, p. 24-39, 2005.

Z. Paiman, "Tepe Narenj: A Royal Monastery on the High Ground of Kabul." Journal of Inner Asian Art and Archaeology, vol. 5, p. 33-58, 2012.

Z. Paiman, "Archaeological Activity in Kabul." In Preserving Cultural Heritage of Afghanistan. Proceedings of The International Conference Held at Kabul University, November 2014, p. 97–106, 2017.

K. S. Park, R. Milke, E. Rybacki and S. Reinhold, "Application of image analysis for the identification of prehistoric ceramic production technologies in the North Caucasus (Russia, Bronze/Iron Age)," Heritage, no. 2, p. 2327-2342, 2019.

C. L. Reedy, "3D documentation and analysis of porosity in deteriorated historic brick", Studies in Conservation, no. 65 (S1) p. 258-261, 2020.

B. Schmid, J. Schindelin, A. Cardona, M. Longair, and M. Heisenberg, "A high-level 3D visualization API for Java and ImageJ," BMC Bioinformatics, vol. 11, no. 1, p. 1–7, 2010. https://doi.org/10.1186/1471-2105-11-274

J. Schindelin, I. Arganda-Carreras, E. Frise, et al. Fiji: an open-source platform for biological-image analysis. Nat Methods 9, 676–682 (2012). https://doi.org/10.1038/nmeth.2019

M. Singh Gill, C. Priego Rendo, and Sreekumar Menon. "Materials and Techniques: Early Buddhist Wall Paintings and Sculptures at Sumda Chun, Ladakh." Studies in Conservation 59, no. 5, p.300–313, 2014. https://doi.org/10.1179/2047058413Y.0000000090

Z. Tarzi, "La technique du modelage en argile en Asie Centrale et au Nord-Ouest de l'Inde sous les Kouchans: la continuité malgré les ruptures." Ktéma 11, p. 57–93, 1986.

K.M. Varma, The Indian Technique of Clay Modelling. Santiniketan: Proddu, 1970.

N. Wang, L. He, E. Egel, S. Simon, and B. Rong. "Complementary Analytical Methods in Identifying Gilding and Painting Techniques of Ancient Clay-Based Polychromic Sculptures." *Microchemical Journal* 114, p. 125–40, 2014. https://doi.org/10.1016/j.microc.2013.12.011

X. Wang, G. Zhen, X. Hao, T. Tong, F. Ni, Z. Wang, J. Jia, L. Li, and H. Tong "Spectroscopic Investigation and Comprehensive Analysis of the Polychrome Clay Sculpture of Hua Yan Temple of the Liao Dynasty, in Spectrochimica Acta

Part A: Molecular and Biomolecular Spectroscopy, Volume 240, p. 1386-1425, 2020. https://doi.org/10.1016/j.saa.2020.118574

D. Wildenschild and A. P. Sheppard, "X-ray imaging and analysis techniques for quantifying pore-scale structure and processes in subsurface porous medium systems," Adv. Water Resour. Volume 51, p. 217-246, 2013. https://doi.org/10.1016/j.advwatres.2012.07.018

FIGURES AND TABLES

Figure 1. Macro-photo of the sample TN7.

Figure 2. Location of the archaeological site of Tepe Narenj (Kabul, Afghanistan). Aerial Photo of the site: Z. Paiman ©

Figure 3. Examples of architectural *terracruda* sculptures preserved in the archaeological site of Tepe Narenj (Kabul, Afghanistan).

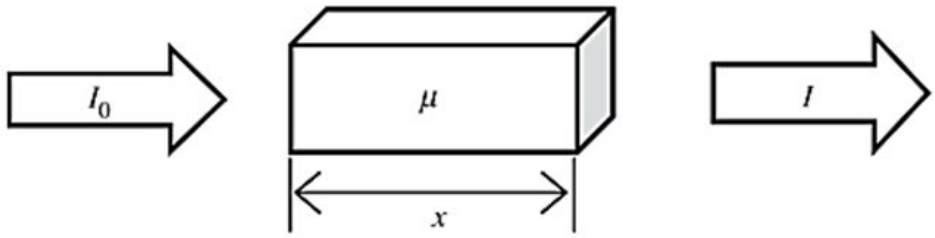

Figure 4. Attenuation of X-rays passing through the sample according to the Beer-Lambert law.

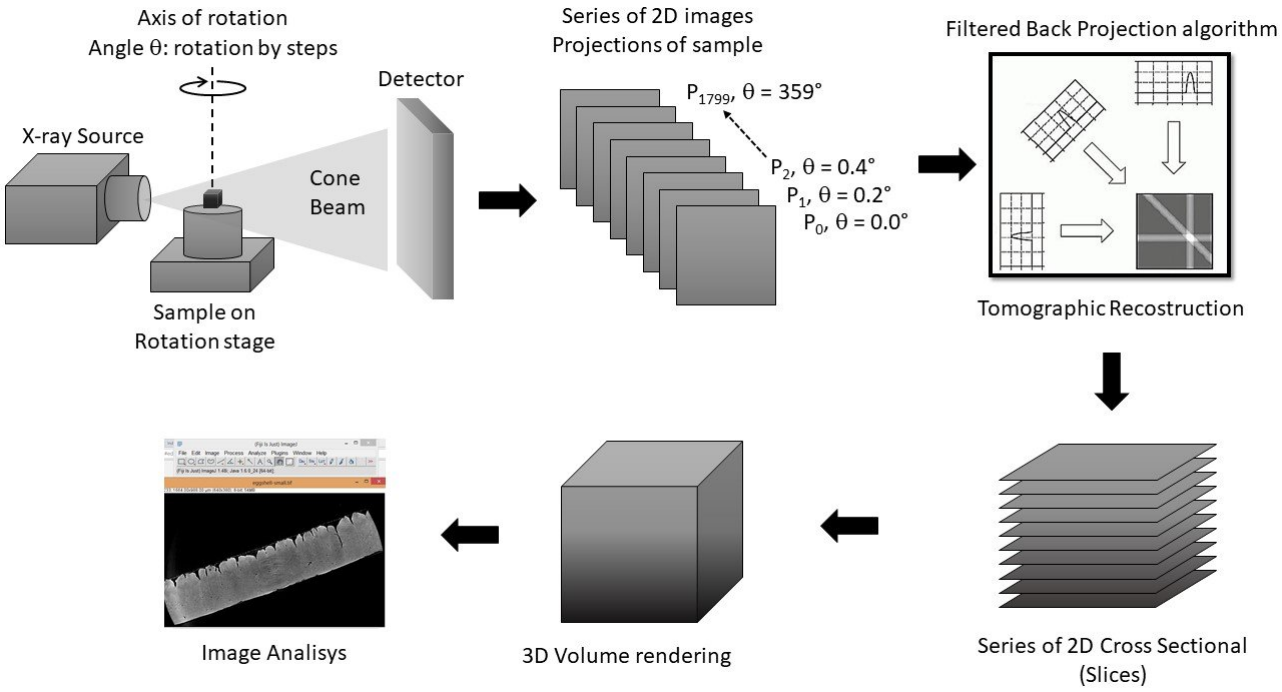

Figure 5. Schematic representation of operations sequence to perform an X-ray microtomography measurement.

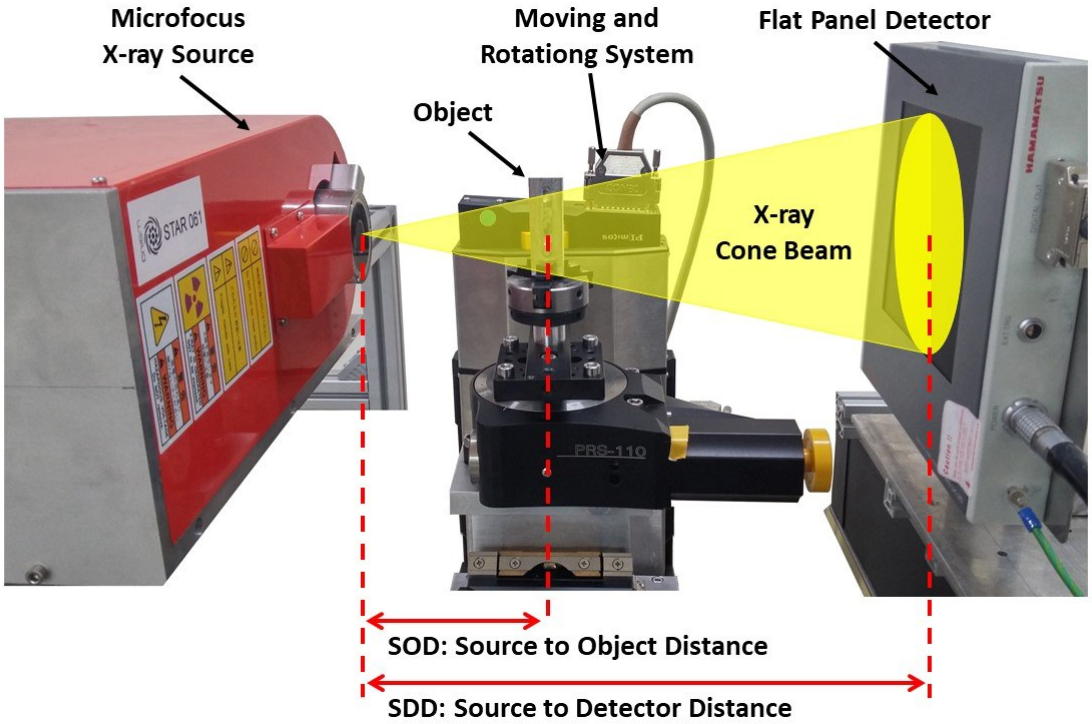

Figure 6. µTomo experimental station @Lab. STAR (University of Calabria, Italy).

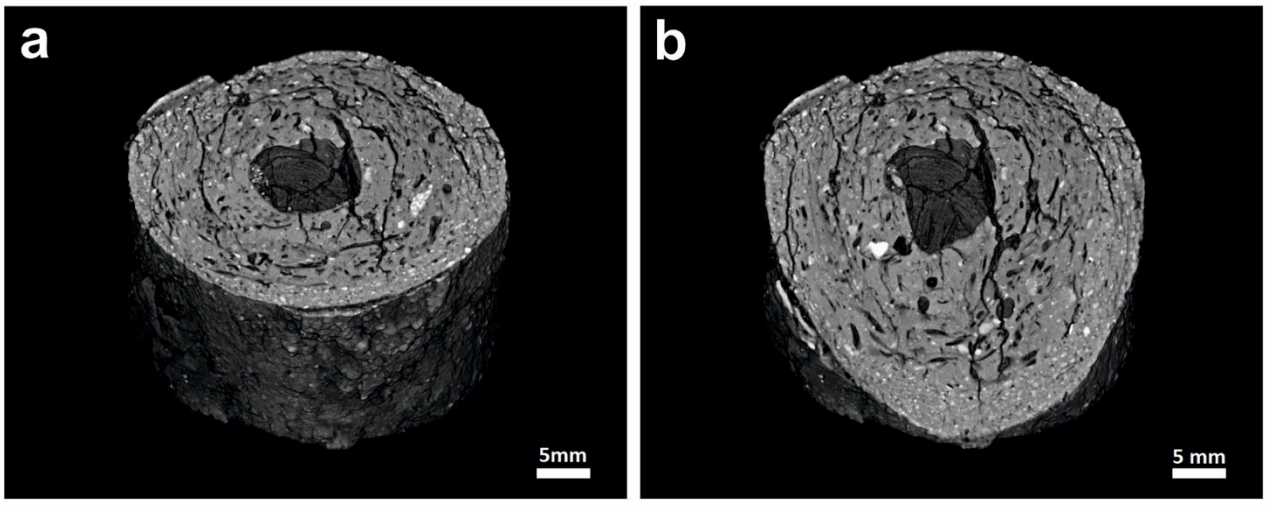

Figure 7. a) 3D rendering of the bulk sample; b) 3D rendering of the bulk sample, cut through an oblique plane.

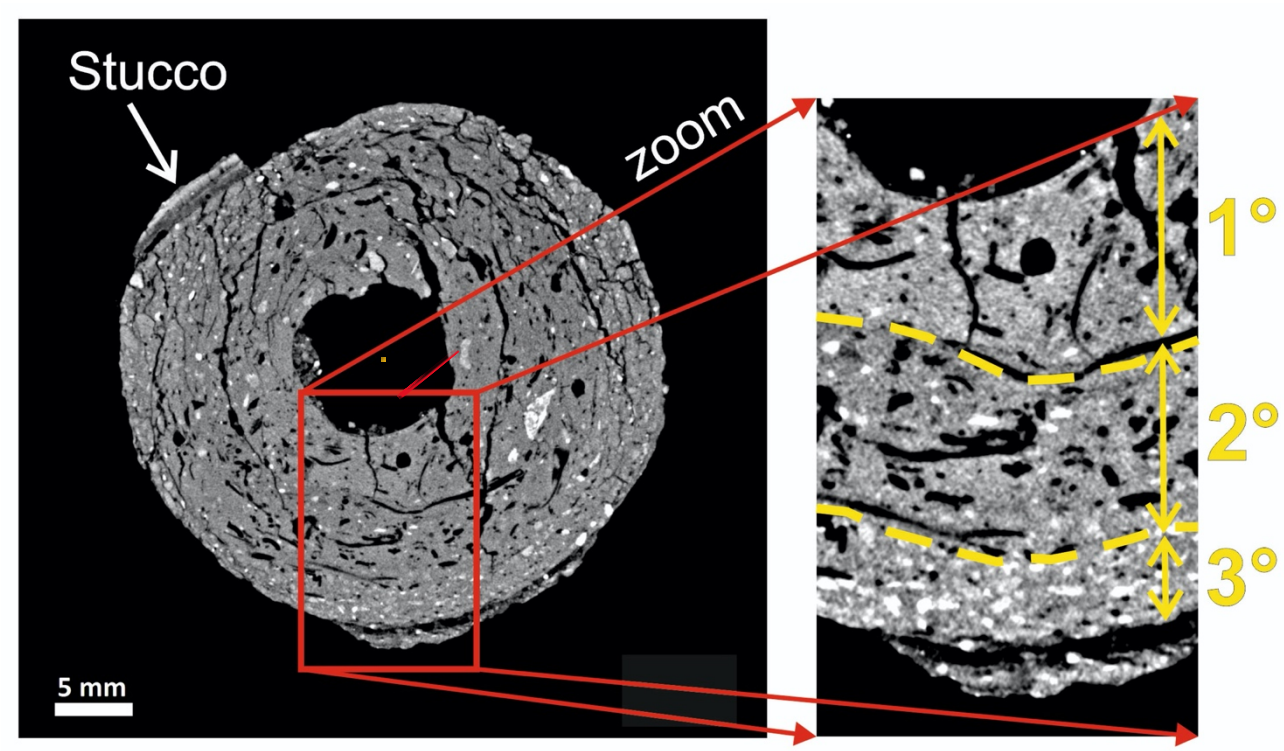

Figure 8. Equatorial section of the sample, with the zoom of the three main layers.

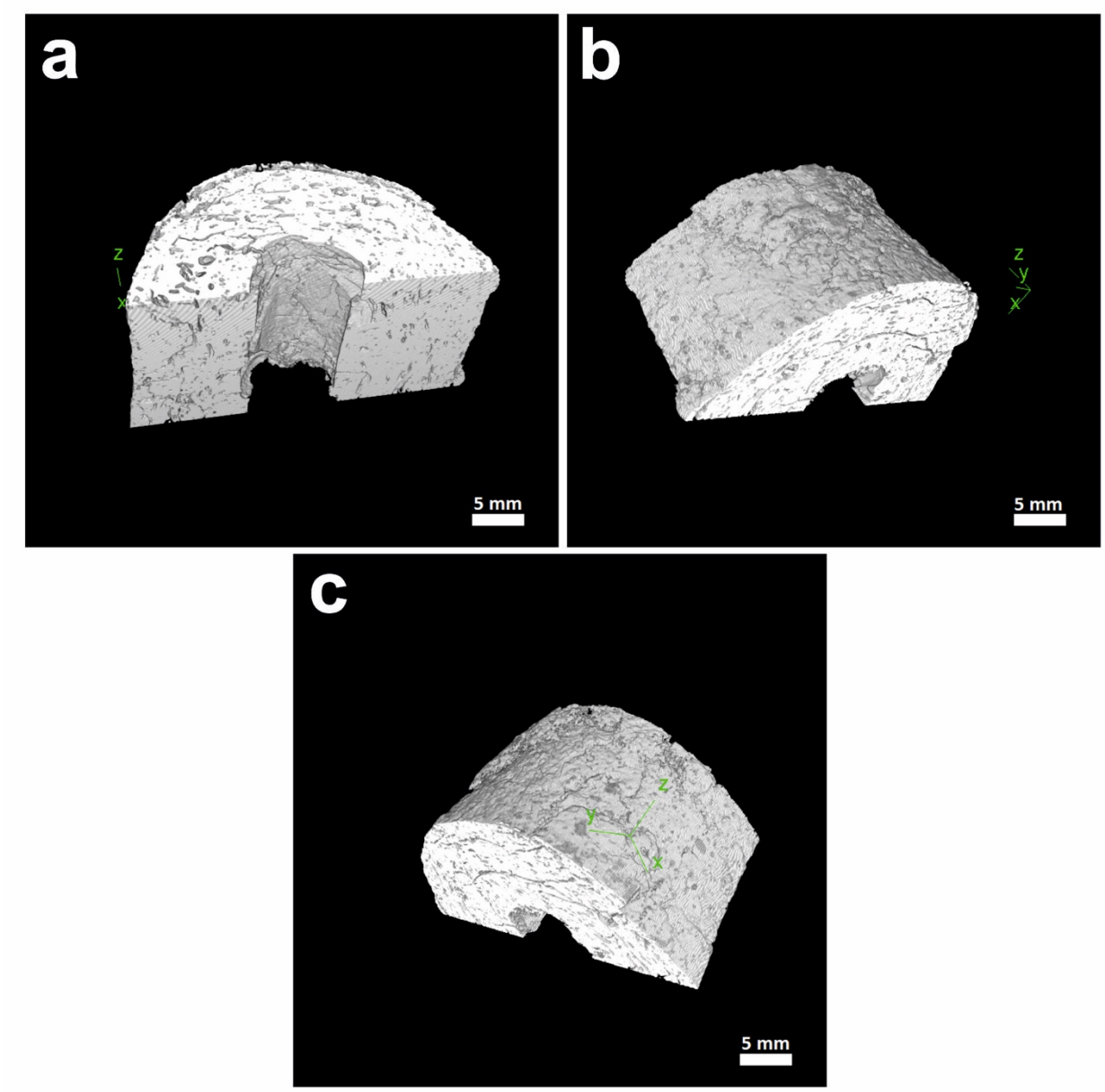

Figure 9. a) 3D rendering of a portion of the clay material (0° position); b) 3D rendering of a portion of the clay material, rotated of 143 degrees from the start position; c) 3D rendering of a portion of the clay material, rotated of 234 degrees from the start position.

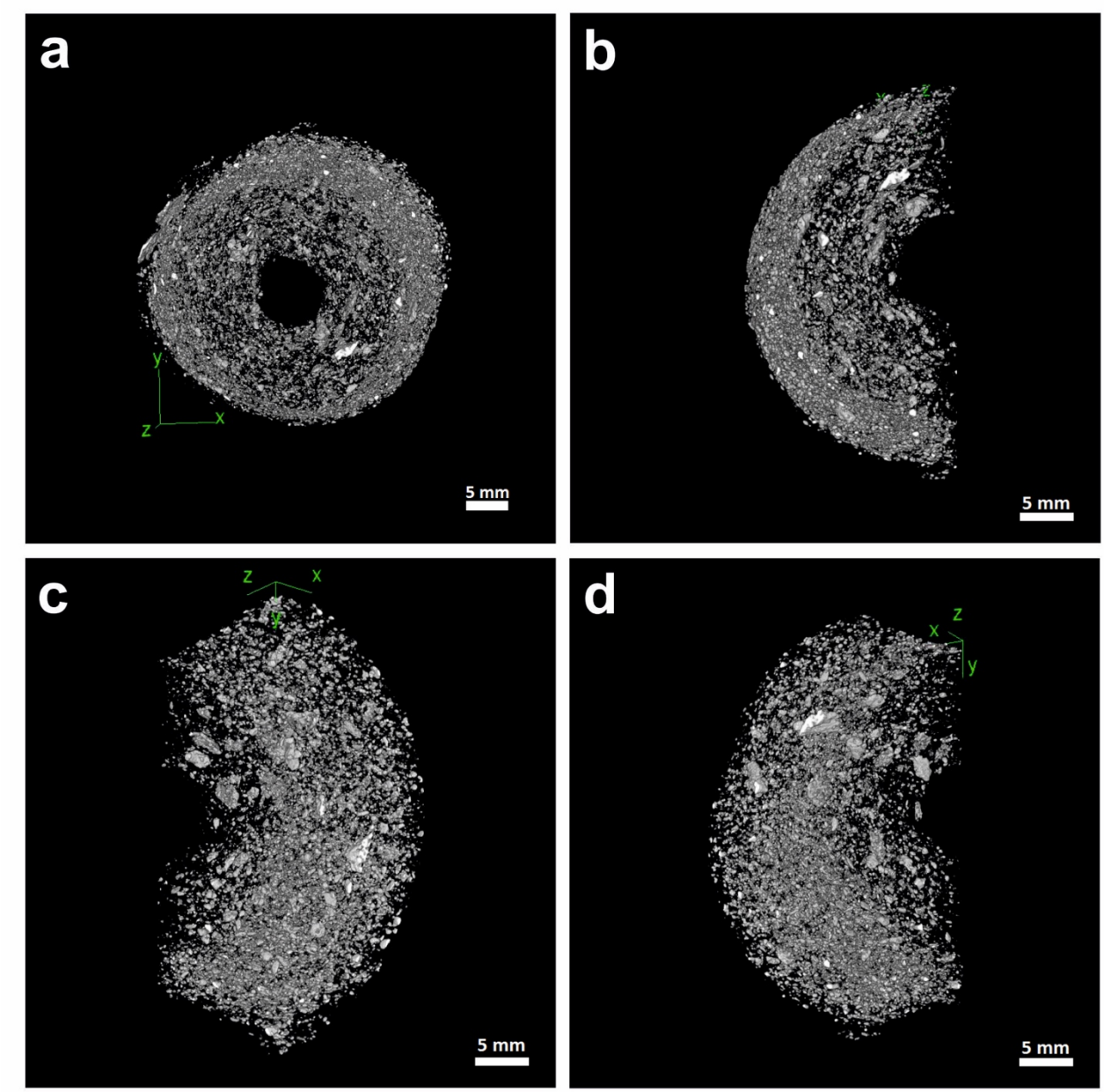

Figure 10. a) 3D rendering of the inert material shown in the equatorial section; b) 3D rendering of a portion of the inert material (0° position); c) 3D rendering of a portion of the inert material rotated of 40 degrees from the start position; d) 3D rendering of a portion of the inert material rotated of 146 degrees from the start position.

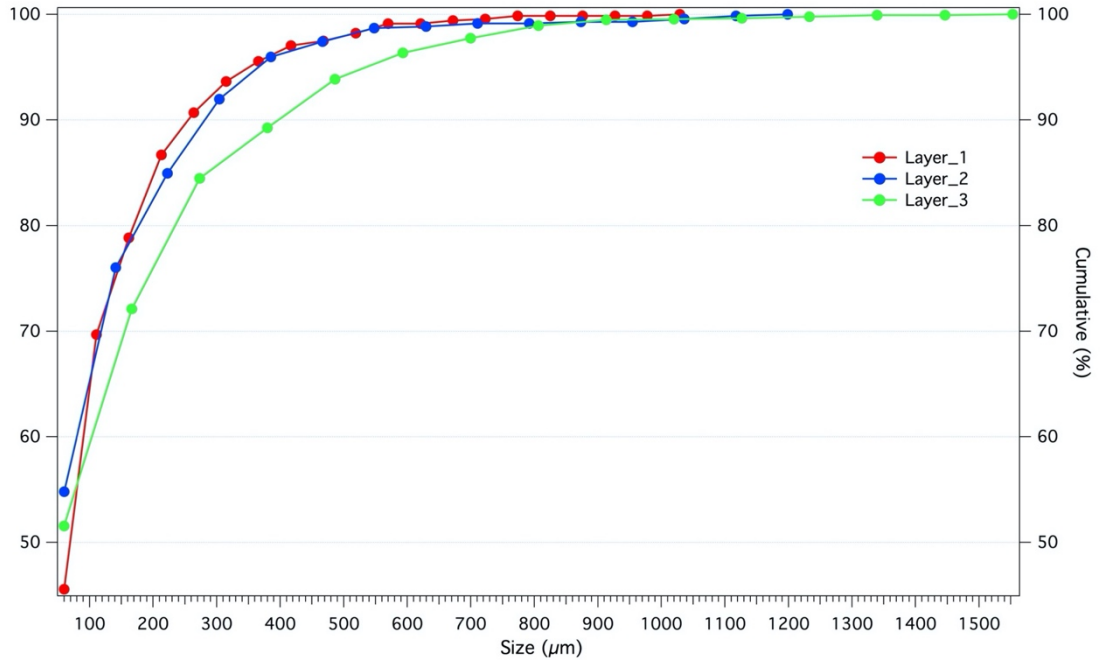

Figure 11. Cumulative frequency curves of the particle size distribution for the inert material inside the layers 1, 2 and 3.

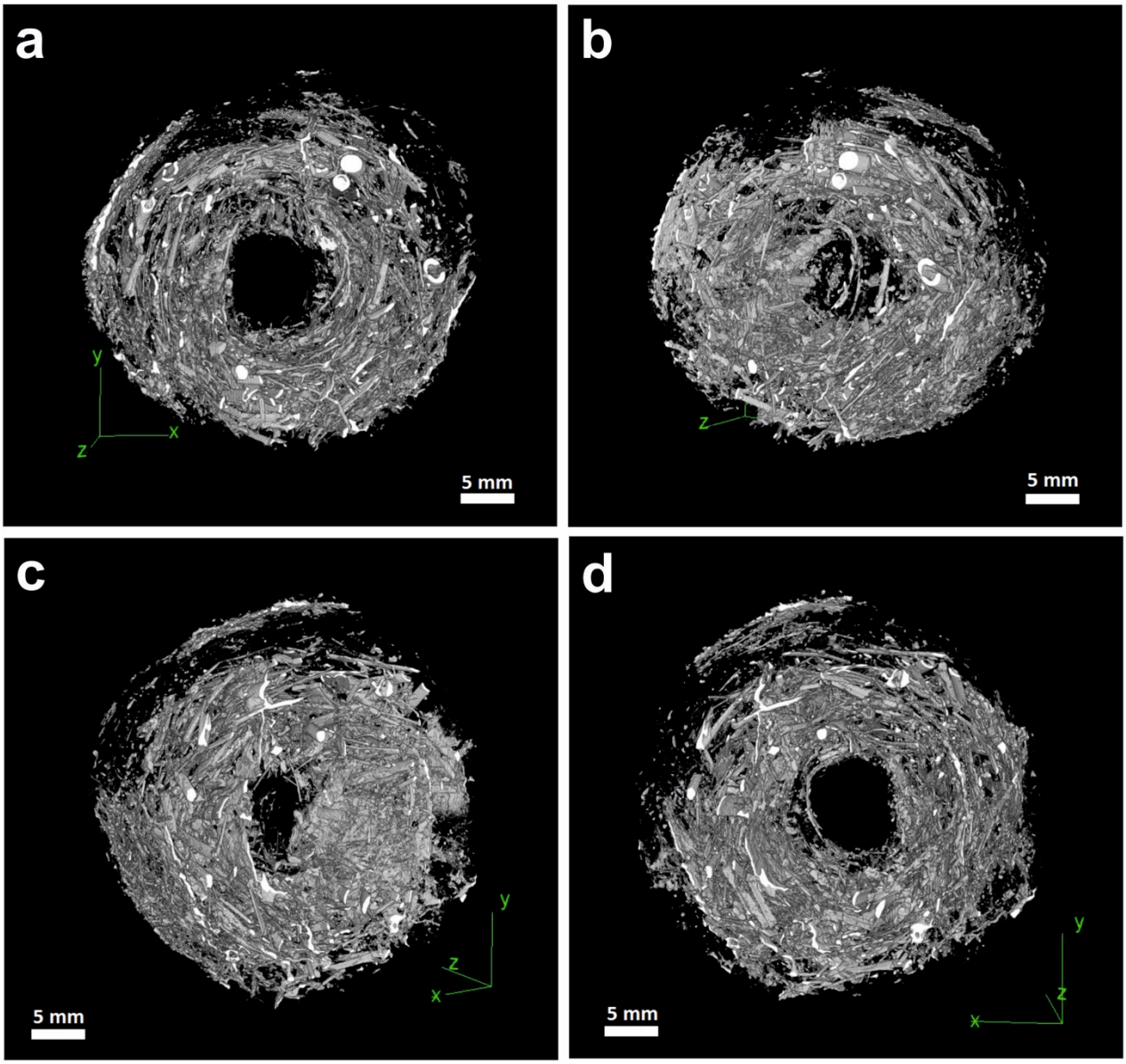

Figure 12. a) 3D rendering of the voids shown in the equatorial section (0° position); b) 3D rendering of the voids rotated of 35 degrees from the start position; c) 3D rendering of the voids rotated of 160 degrees from the start position; d) 3D rendering of the voids rotated of 193 degrees from the start position.

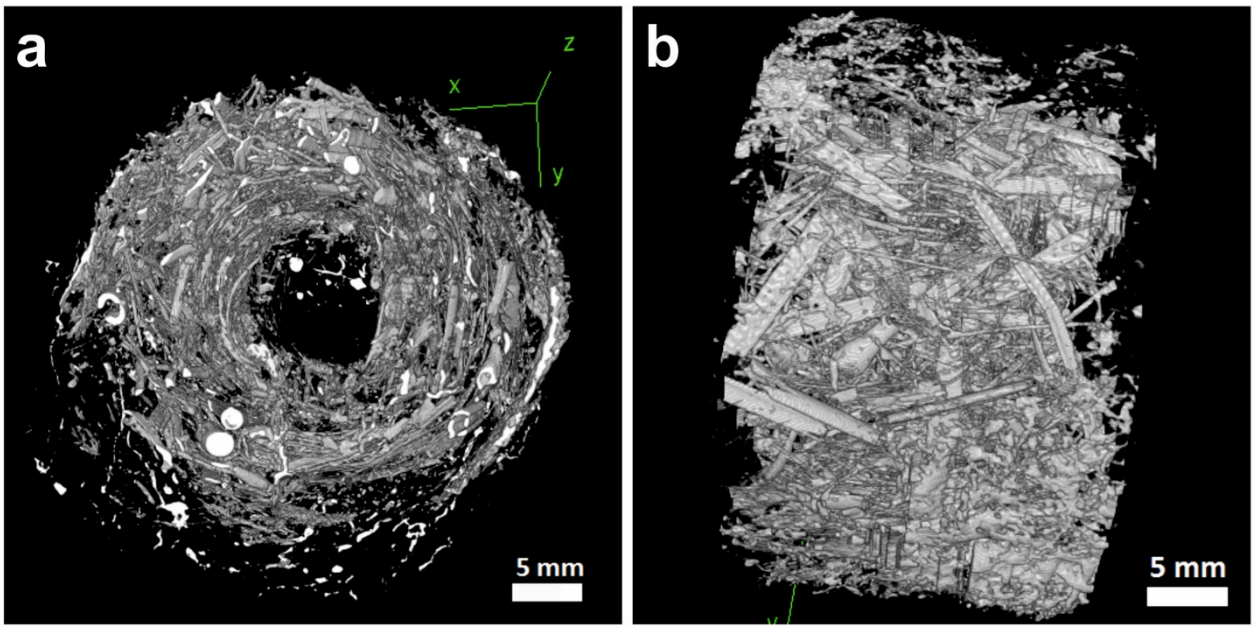

Figure 13. a) 3D rendering of the voids shown in the equatorial section; b) 3D rendering of the voids rotated of 90 degrees from the equatorial position.

Figure 14. Dayal Pal, sculptor from the Kumortuli clay artists' quarter (Kolkata, West Bengal) showing the finger modelling process. On the right, detail of the fingers next to the clay and jute fibres used in the procedure.

Parameter	Specification	Unit
Pixel size	50 × 50	μμ
Photodiode active area	115 × 115	mm
Number of active pixel	2316 × 2316	pixels

Table 1. Detector features.

Microfocus source parameters	
X-ray tube voltage (kV)	130
X-ray tube current (μA)	76
X-ray focal spot mode Small	7μm
Power (W)	9.88
Energy filter	100μm of Cu
Source and detector position	
Source to Object Distance - SOD (mm)	200
Source to Detector Distance - SDD (mm)	500
Magnification	2.5
Equivalent pixel-size (μm)	20
Detector parameters	
Number of images captured	1800
Angular step (°)	0.2
Acquisition time (ms)	2000

Table 2. Measurement parameters.

Sample TN7	Intert materials (% 3D volume)	Clay material (% 3D volume)	Void (% 3D volume)	Max. size of the inert materials (μm)	Mean size of the inert materials (μm
Layer 1	1.81%	92.71%	5.48%	1500	264
Layer 2	1.64%	87.29%	11.07%	1280	166
Layer 3	4.53%	90.38%	5.09%	1660	202

Table 3. Estimation of the percentage of the clay material, inert material and voids in the layers 1, 2 and 3 of the sample TN7.